Available online at www.sciencedirect.com
SCIENCE DIRECT®
Combustion and Flame 144 (2006) 24–36
Combustion and Flame
www.elsevier.com/locate/combustflame

Linear time reduction of large kinetic mechanisms with directed relation graph: *n*-Heptane and iso-octane

Tianfeng Lu *, Chung K. Law

Department of Mechanical and Aerospace Engineering, Princeton University, Princeton, NJ 08544, USA

Received 7 September 2004; received in revised form 30 January 2005; accepted 10 February 2005

Available online 30 August 2005

Abstract

The algorithm of directed relation graph recently developed for skeletal mechanism reduction was extended to overall linear time operation, thereby greatly facilitating the computational effort in mechanism reduction, particularly for those involving large mechanisms. Together with a two-stage reduction strategy and using the kinetic responses of autoignition and perfectly stirred reactor (PSR) with extensive parametric variations as the criteria in eliminating unimportant species, a detailed 561-species *n*-heptane mechanism and a detailed 857-species iso-octane mechanism were successfully reduced to skeletal mechanisms consisting of 188 and 233 species, respectively. These skeletal mechanisms were demonstrated to mimic well the performance of the detailed mechanisms, not only for the autoignition and PSR systems based on which the reduced mechanisms were developed but also for the independent system of jet-stirred reactor. It was further observed that the accuracy of calculated species concentrations was equivalently bounded by the user-specified error threshold value and that the reduction time for a single reaction state is only about 50 ms for the large iso-octane mechanism.

Keywords: Directed relation graph; Reduced mechanism; *n*-Heptane; Iso-octane

1. Introduction

Chemical kinetics of fuel oxidation is an integral component of combustion phenomena. However, because of the complexity and strong nonlinearity of the reaction pathways and the associated reaction rates for the myriad of reactions and species involved, computational simulations with detailed mechanisms have been limited to the simplest fuels such as hydrogen and the lower hydrocarbons in idealized flow fields. The simulation is further complicated by the existence of highly reactive radicals which induces significant stiffness to the governing equations due to the dramatic differences in the time scales of the species. Consequently, there exists the need to develop from these detailed mechanisms corresponding reduced mechanisms of fewer variables and moderated stiffness, while maintaining the accuracy and comprehensiveness of the detailed mechanism.

A major category of previous reduction methods was based on time scale analysis, through which both the number of variables and the stiffness can be reduced by eliminating short time scales associated with quasi-steady-state species or partial equilibrium reactions [1–8]. The method of intrinsic low-dimensional manifold [9] performs eigenvalue analysis of the Jacobian matrix and assumes that the fast subspace van-

* Corresponding author. Fax: +1 609 258 6233.
E-mail address: tlu@princeton.edu (T. Lu).

0010-2180/$ – see front matter
doi:10.1016/j.combustflame.2005.02.015

ishes quickly. The frequently reused reaction conditions are handled with the method of in situ adaptive tabulation to reduce the overall simulation cost [10,11]. The theory of computational singular perturbation (CSP) considers the time dependence of the Jacobian matrix, and higher-order accuracy can be obtained [12–16].

While time scale analyses can reduce the number of species and the stiffness by eliminating species or reactions with short time scales, significant overhead in central processing unit (CPU) cost is typically involved in solving the algebraic equations obtained by assuming that the fast species or reactions are exhausted, particularly when the size of the mechanism is large. Therefore, it is frequently necessary to identify and eliminate the unimportant species and reactions, i.e., to perform the skeletal reduction, before reduction based on time scale analysis is conducted.

Various methods for skeletal reduction have been developed. One of the earliest developed methods for skeletal reduction is sensitivity analysis [17–19], which is simple to apply. However, it does not directly provide decoupled information about the reactions and species, and further postprocessing is required. The method of principal component analysis (PCA), based on sensitivity analysis, operates on the sensitivity matrices and systematically identifies the redundant reactions [20]. A major restriction of algorithms based on sensitivity analysis is that they are time consuming to compute the sensitivity matrices for large mechanisms.

Reaction elimination can also be performed using optimization approaches, such as integer programming, aiming to obtain an optimal set of reactions for given constraints [21]. While the optimal set of reactions can be identified, the optimal solution strictly depends on the selection of constraints, which is frequently quite involved. Furthermore, the optimization approach is asymptotically slower than sensitivity analysis, since integer programming is in general an NP-hard problem. Another method, the detailed reduction [22], provides a fast way for the identification of unimportant reactions by directly comparing the reaction rates with a preselected critical value. The restriction of this method is the lack of consideration of species or reaction coupling, because of which a slower reaction is not always unimportant, particularly when it involves crucial radicals. Consequently, significant human interaction and extensive validation may be required.

While skeletal reduction based on reaction elimination has been extensively studied, those methods involving direct species elimination are less established. A method was developed for the identification of unimportant species by resolving species coupling using Jacobian analysis [23]. The coupling among species is formulated with the entries of the Jacobian matrix and the species that are strongly coupled with the major species are identified iteratively. This method is practically faster than those based on sensitivity analysis, although formulation of the species coupling using Jacobian matrix is nontrivial and system-dependent knowledge is frequently required.

In a recent work [24], the method of directed relation graph (DRG) was developed to identify unimportant species by resolving species coupling with high efficiency and minimal requirement of system-dependent knowledge. In the present investigation this method was extended to the reduction of large mechanisms with hundreds of species, namely those for n-heptane and iso-octane [25,26], and the efficiency and accuracy of this extended method were demonstrated and analyzed.

2. Methodology

2.1. DRG method

The skeletal reduction is to identify and eliminate unimportant reactions or species. Typically, the identification of unimportant species is more involved than that of reactions due to the complex coupling of the species. The method of DRG was developed to resolve species coupling efficiently, by starting with direct species coupling, which indicates that the removal of one species B from the mechanism induces immediate error to the production rate of another species A. Such immediate error, noted as r_{AB}, can be expressed as

$$r_{\mathrm{AB}} \equiv \frac{\sum_{i=1,I} |\nu_{\mathrm{A},i}\omega_i \delta_{\mathrm{B}i}|}{\sum_{i=1,I} |\nu_{\mathrm{A},i}\omega_i|},$$

$$\delta_{\mathrm{B}i} = \begin{cases} 1, & \text{if the } i\text{th reaction involves} \\ & \text{species B,} \\ 0, & \text{otherwise,} \end{cases} \tag{1}$$

where the subscripts A and B indicate the species identity, i is the ith reaction, $\nu_{\mathrm{A},i}$ the stoichiometric coefficient of species A in the ith reaction, and ω the reaction rate. The terms in the denominator are the contributions of the reactions to the production rate of species A, and the terms in the numerator are those in the denominator that involve species B. If the relative error r_{AB} is not small compared to a threshold value ε, the removal of species B from the skeletal mechanism immediately induces a nonnegligible error in A. Consequently species B should be kept in the skeletal mechanism if species A is to be retained. Such an immediate requirement of species A to species B is denoted as $\mathrm{A} \rightarrow \mathrm{B}$.

Species can also be coupled indirectly through direct coupling with intermediate species. For example, if A → B and B→C, then A requires C indirectly. The set of species required either directly or indirectly by species A is defined as the dependent set of A, and it is readily seen that if species A is to be retained in the skeletal mechanism, so should be all the species in its dependent set. Therefore, for a given set of major species which must be retained in the skeletal mechanism, the species of the skeletal mechanism can be obtained from the union of all the dependent sets of the major species. The dependent set of a major species can be identified efficiently by mapping the species coupling to a directed relation graph, which can be constructed using the following rules:

(1) Each vertex in DRG is uniquely mapped to a species in the detailed mechanism.
(2) There exists a directed edge A → B if and only if $r_{AB} \geqslant \varepsilon$.
(3) The starting vertices of DRG correspond to the major species in the mechanism.

A sample configuration of DRG is shown in Fig. 1a, in which vertices A, B, ..., F correspond to the respective species, and each directed edge indicates an immediate requirement of one species of another. The starting vertex A, enclosed in a bold circle, is a major species in the mechanism. The skeletal species in Fig. 1a correspond to all the vertices reachable from the starting vertex. Graph searching methods such as depth first search (DFS) can thus be exploited to efficiently find all the vertices reachable from the starting one. Species A, B, and D are therefore identified as the species of the skeletal mechanism in the current example.

It is noted that the set of starting vertices does not need to contain every major species in the mechanism. Instead, in most cases, it is sufficient to start from a single species, such as the fuel, to identify all the species in the skeletal mechanism. This is because the other major species such as the oxidizer, the products, and the major radicals are required by the fuel either directly or indirectly, and as such they can be retained together with the other important species automatically in the DFS. The inert species can be either added back to the skeletal species set after the DRG reduction since they will be eliminated in the DRG reduction or included as a starting species for DRG reduction such that they can be retained consequently. In cases in which multiple starting vertices are required, a DFS can be applied to each starting vertex and, as mentioned above, the collection of all the discovered vertices constitutes the species set of the skeletal mechanism. After the skeletal species are identified, reactions involving any of the eliminated species are removed and the skeletal mechanism is generated.

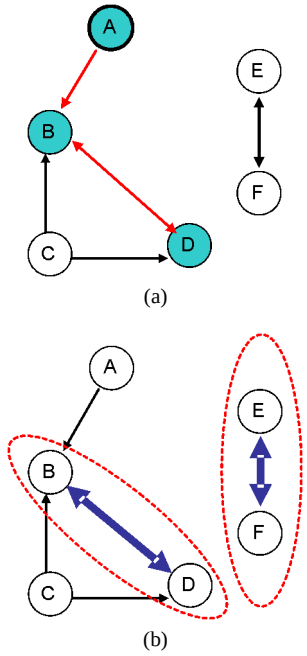

Fig. 1. Schematics showing typical configuration of the directed relation graph (DRG); the vertices correspond to the species and the directed edges correspond to the immediate requirement of one species to another. (a) Basic configuration and identification of skeletal species. (b) Demonstration of strongly coupled species groups.

An important observation of skeletal reduction with DRG is the existence of strongly coupled species groups, which are characterized by relatively stronger intragroup coupling than intergroup coupling. A schematic of strongly coupled species groups is shown in Fig. 1b. For example, the intragroup couplings in the species groups {B, D} and {E, F} are stronger than the intergroup couplings. Such strongly coupled species groups should be either retained or eliminated together from the skeletal mechanism. Consequently, the elimination of a strongly coupled species group induces a jump in the number of species in the skeletal mechanism as the error threshold value ε increases, as was shown in the reduction of a detailed ethylene mechanism [24]. Such jumps in the species number can significantly reduce the possible number of candidate skeletal mechanisms and thereby reduce the amount of effort for skeletal mechanism validation.

To obtain a skeletal mechanism over a sufficiently wide range of parameters such as pressure, temperature, equivalence ratio, and residence time, a set of reaction states are sampled from typical applications such as perfectly stirred reactor (PSR) and autoigni-

tion. A local DRG reduction can be performed for each of these reaction states, and the union of the species sets of all the local skeletal mechanisms yields the species set of the global skeletal mechanism.

It is to be noted that since the comprehensive skeletal mechanism developed here is the union of a set of local skeletal mechanisms each developed for a reaction state, many partially comprehensive skeletal mechanisms can be developed through the union of any number of these local skeletal mechanisms, with different sizes, different parametric ranges, and different extents of computational cost reduction. The methodology is therefore applicable to the development of mechanisms of various degrees of comprehensiveness. Indeed, each of the local skeletal mechanisms being applicable to a given reaction state allows the ultimate potential of transition between different skeletal mechanisms during a simulation, from state to state—a promising prospect that is worth further pursuing.

2.2. Extended DRG algorithm for linear time reduction

The major advantage of DRG reduction is that the entire reduction can be completed in a time that is linearly proportional to the number of reactions in the mechanism. Linear time reduction is crucial for applications requiring real time or case-specific reduction. In CFD simulations using explicit integration schemes, real time reduction based on Jacobian or sensitivity matrix analysis requires significant overhead, which consequently diminishes the efficiency of the reduction. In such cases, a reduction algorithm with linear reduction time is required to minimize the overhead and provide the highest efficiency. DRG is such an algorithm in that the entire reduction time is linearly proportional to the number of reactions in the mechanism, as will be shown in the following section.

There are three major steps in DRG reduction, namely the graph construction step using Eq. (1), the graph searching step to identify the skeletal species, and the skeletal mechanism generation step to create the final mechanism files.

The graph construction step involves evaluation of the relative errors for each pair of species according to Eq. (1). There are totally K^2 terms to be evaluated, where K is the number of species, and each term contains $O(I)$ multiplications. Therefore a brute-force approach in graph construction would require $O(K^2 I)$ evaluations, which can be asymptotically more expensive than the evaluation of the Jacobian matrix. However, the stoichiometric coefficient matrices for the detailed mechanisms are sparse in general; i.e., the number of species involved in each elementary reaction is bounded by a small constant number $S_{\max}$, say 6–8. Thus graph construction can be performed in a more efficient way by evaluating only the contributions of each reaction to the related edges. Since each reaction involves at most $S_{\max}$ species, the maximum number of edges in the graph is bounded by a linear function of I and so is the time complexity of the graph construction step. The detailed procedure for graph construction is shown in the coarse-grain pseudo code in Fig. 2.

In the second step, each edge in the graph can be compared with the threshold value ε for truncation. The resulting graph with a smaller number of edges can be searched with DFS to obtain the final species set of the skeletal mechanism. Since the number of edges is bounded by a linear function of I, and DFS features a linear searching time proportional to the number of edges in the graph, the time complexity of the second step is also $O(I)$. While this standard graph searching method is fast for reduction with given accuracy requirement, it is not sufficient if the number of species, instead of the accuracy, is given for the reduction. In such cases, the DFS algorithm can be revised such that species can be sorted by the critical value of ε.

The revised DFS (RDFS) method first sorts the edges by their respective values r. Then the edges are inserted into the initially empty graph in decreasing order of r, such that the strongly coupled species groups, or kernels, can be formed first. The kernels grow larger as more edges are inserted into the graph, until a bridging edge is inserted and an otherwise isolated kernel becomes reachable from the starting vertices. The r value of this bridging edge then becomes the critical ε value for each species in this kernel. The procedure continues until all the edges are inserted, as described in Fig. 2. While general purpose sorting algorithms take $O(I \log I)$ time to sort the edges, a simple linear time bucket sorting algorithm can be applied in the RDFS algorithm, considering that the possible value of an edge is between 0 and 1, and the r value needs to be accurate only to 10^{-3}–10^{-4}. The graph searching time for the RDFS algorithm is therefore still a linear function of I by the argument that the total number of edges is $O(I)$ and no edge needs to be searched more than once. Compared with the regular DRG reduction, the extended DRG provides the sorted species list in a single linear time RDFS search. Therefore the skeletal mechanism of any given accuracy or number of species can be generated using this list.

Finally, the third step of the DRG reduction is to eliminate the reactions that involve any removed species and subsequently generate the final skeletal mechanism. This step is straightforward and it is trivial to show that the time complexity is also $O(I)$,

```
DRG()
    # Step 1: Graph Construction
    For each reaction i = 1 : I
        For each species pair A, B involved in reaction i,
            Evaluate the term ν_{A,i}ω_i and δ_{B,i}
            If edge A→B has not been initialized
                Reset the numerator and denominator of r_AB for edge A→B
            End if
            Modify the numerator and denominator of r_AB correspondingly
        End for
    End for
    For each initialized edge
        Evaluate r_AB with the accumulated numerator and denominator
    End for

    # Step 2: Graph Searching
    Call RDFS()

    # Step 3: Create Skeletal Mechanism
    Eliminate species with marked values smaller than ε
    Eliminate reactions involving eliminated species
    Write the retained species and reactions to the skeletal mechanism
End

RDFS()
    Bucket sort the edges in decreasing order of r
    Initialize an empty graph with only vertices
    Mark the starting vertices with unity and the other species with zero
    For each edge A→B in the sorted list
        Insert A→B into the graph in decreasing order of r
        If A is marked and B is not marked
            Depth first search with B as root,
                and mark every newly discovered vertex with value r_AB
        End if
    End for
    Bucket sort the species by their marked value
End
```

Fig. 2. Coarse-grain pseudo code of the extended DRG method with linear time graph construction and revised depth first search (RDFS) algorithm.

provided that the number of species in each reaction is bounded by a constant value, $S_{\max}$.

Since each of the three steps in DRG reduction can be performed in linear time, the overall reduction time for DRG is $O(I)$, i.e., a linear function of the number of reactions in the detailed mechanism.

2.3. Two-stage DRG for reduction of large mechanisms

When the number of species is large in the detailed mechanism, the number of species eliminated by a DRG reduction is expected to be correspondingly large. Consequently, the r value for each pair of the retained species can be changed due to the elimination of the unimportant species. Although the change in the r values is a second-order effect, it is still possible that some species in the skeletal mechanism can be further eliminated if a second-stage DRG is performed on the skeletal mechanism. In such cases, a two-stage DRG reduction can produce a skeletal mechanism slightly smaller than that from a single-stage DRG reduction. The first stage of DRG reduction is the major reduction stage, in which a significant number of species are eliminated from the detailed mechanism, and the second stage is a minor stage whose execution is optional.

While it might be argued that more than two DRG stages are needed to obtain a converged skeletal species set for extremely large mechanisms, it is reasonable to expect, and indeed was found for the reduction of the largest mechanisms currently available such as those of n-heptane and iso-octane [25,26], that a two-stage DRG reduction is quite adequate. It is further noted that, since the second stage of DRG reduction can also be performed in linear time and since the number of reactions in the skeletal mechanism determined from the first DRG reduction stage is

typically much smaller than that of the detailed mechanism, the inclusion of an additional DRG stage does not increase the overall reduction time significantly. Consequently, a slightly smaller skeletal mechanism can be obtained by implementing the second stage with a slightly increased reduction time. Indeed, considering the minuscule amount of time involved in the reduction, as will be shown later, the implementation of the second stage of reduction is entirely appropriate.

With the above extended DRG method, skeletal mechanisms with desired accuracy or size can be generated. While such a skeletal mechanism already has reduced number of species and reactions, there still could be some unimportant reactions that contribute negligibly to every species in the skeletal mechanism. To identify such unimportant reactions, methods based on reaction elimination discussed in the Introduction can be used. For example, a reliable and efficient method using the CSP importance index, which measures the normalized contribution of a reaction to the production rate of a species, can be found in [14,15].

In the next sections, the DRG method will be applied to derive skeletal mechanisms of two large detailed mechanisms for *n*-heptane and iso-octane. The efficiency and accuracy control will be demonstrated and analyzed.

3. Skeletal mechanisms for *n*-heptane and iso-octane

3.1. Skeletal mechanism for *n*-heptane

n-Heptane is an important reference gasoline fuel, and many detailed mechanisms for its oxidation have been developed by different groups [25–31]. Due to the large molecule size, the oxidation process for *n*-heptane is significantly more complex than that of lower hydrocarbons such as methane and ethylene. Furthermore, *n*-heptane exhibits the negative temperature coefficient (NTC) and the two-stage or multi-stage ignition [32] behaviors in the low-temperature regime, whose descriptions require additional sets of reaction pathways. Therefore, the size of the detailed *n*-heptane mechanisms is typically much larger than that of the smaller hydrocarbons. For example, the detailed mechanism developed by Curran et al. [25–27] contains more than 500 species and 2000 elementary reactions. While detailed mechanisms of such a large size can still be used in the simulation of many homogeneous combustion phenomena, they can rarely be applied to the simulation of diffusive systems without significant reduction in size. Indeed, several reduced mechanisms of *n*-heptane have been developed

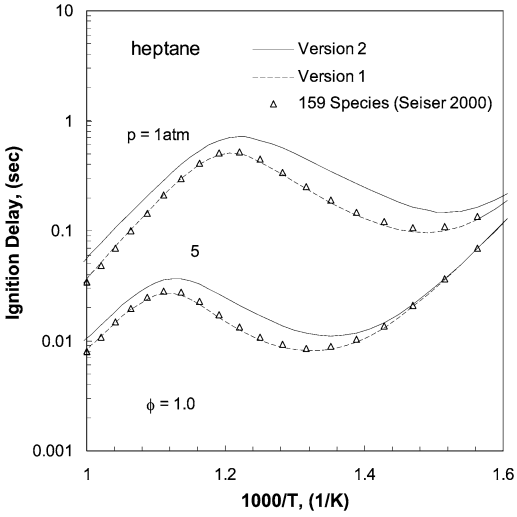

Fig. 3. Comparison of ignition delay around NTC zone for stoichiometric *n*-heptane mixture at atmospheric pressure calculated with different versions of detailed mechanisms and a reduced mechanism, showing the large discrepancy of Versions 1 and 2 of the detailed mechanism and the necessity for updating the skeletal mechanism.

in previous works [33–35]. However, the reduction processes using traditional reduction methods such as sensitivity analysis are typically time consuming. Furthermore, continuous discovery of new information on the reaction pathways results in the frequent updating of the detailed mechanisms, which in turn necessitate corresponding updating of the reduced mechanisms. We demonstrate this point by showing in Fig. 3 that while the skeletal mechanism in [34] agrees well with Version 1 of the detailed mechanism [25], a large discrepancy in the computed ignition delay time is observed when the detailed mechanism is updated to Version 2 [26,27], hence indicating the need for the development of a new skeletal mechanism for the updated detailed mechanism. In such a case, the DRG method can be applied for the fast reduction of large mechanisms whenever they are updated.

We have thus applied the two-stage DRG method with the RDFS algorithm to Version 2 of the 2002 detailed *n*-heptane mechanism [25,26], posted on the LLNL website [27]. This detailed mechanism consists of 561 species and 2539 reactions. Typical working conditions were sampled from PSR and autoignition with the equivalence ratio ranging from 0.5 to 1.5, and the pressure ranging from 1 to 40 atm. The initial temperature for PSR was fixed at 300 K and the residence time range was from the state of extinction to that of near equilibrium. The initial temperature range for autoignition was from 600 to 1800 K, which covers both the low-temperature NTC regime and the high-temperature ignition regime. More than 1000 points

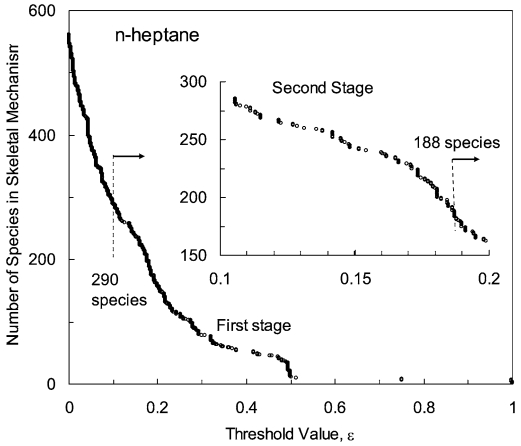

Fig. 4. Dependence of number of species in the skeletal mechanism as a function of the user-specified error threshold value ε for the first and second stages of global DRG reduction for n-heptane mixture, based on densely sampled reactions states from PSR and autoignition for pressure from 1 to 40 atm, equivalence ratio from 0.5 to 1.5, initial temperature range from 600 to 1800 K for autoignition, and 300 K for PSR.

were sampled to ensure the coverage of every representative reaction condition. The entire reduction process using these sample reaction states took a few seconds, which is negligible compared to the simulation time.

The number of species in the skeletal mechanism as a function of the critical relative error ε for the first and second DRG reduction stages is shown in Fig. 4. It is seen that, from the first stage of reduction, the number of species decreases rapidly as ε increases when ε is small, say less than 0.2, while further increasing the value of ε leads only to slight reductions in the species number. This trend implies that significant numbers of species can be eliminated from the detailed mechanism even with a small ε value, i.e., with high accuracy. By choosing an $\varepsilon = 0.1$, 290 species are retained after the first stage of reduction. It may be noted that, because of the large number of total species involved, jumps in the species number representing the elimination of strongly coupled groups consisting of 10 to 20 species are not sharply contrasted on the graph.

The second DRG reduction was then conducted based on the 290-species first-stage skeletal mechanism. Facilitated by the species number jumps in the reduction curve at this stage, $\varepsilon \sim 0.19$ was selected and a 188-species skeletal mechanism was generated. After further elimination of unimportant reactions using the CSP importance index, a final skeletal mechanism with 842 reactions was obtained. The size of this skeletal mechanism is close to that in the previous reduction [34], which has 159 species and 770 reactions.

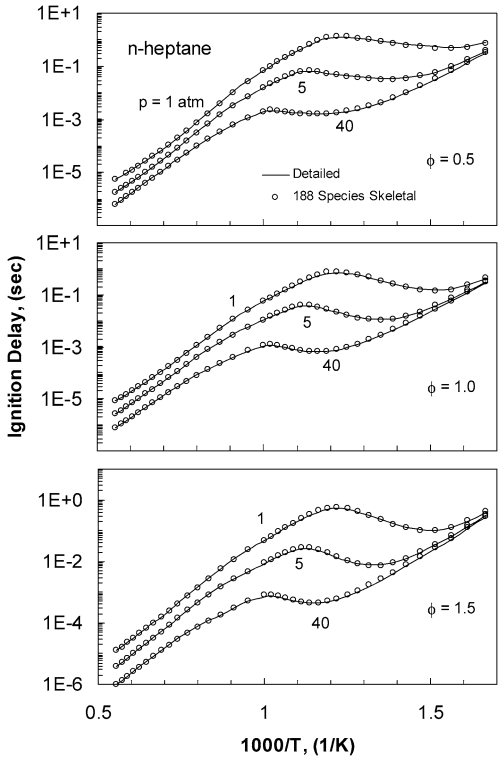

Fig. 5. Comparison of calculated ignition delay of n-heptane/air mixture autoignition as a function of initial temperature under constant pressure and constant enthalpy with detailed and 188-species skeletal mechanisms, for equivalence ratio from 0.5 to 1.5, pressure from 1 to 40 atm, and initial temperature from 600 to 1800 K.

The 188-species skeletal mechanism was validated against the detailed one for PSR and autoignition within the parameter range of the reduction. Fig. 5 shows the calculated ignition delay time of heptane/air mixtures as a function of the initial temperature for $\phi = 0.5$–1.5 and $p = 1$–40 atm. It is seen that the agreement between the skeletal and the detailed mechanisms is good for both the NTC and the high-temperature regimes. Fig. 6 compares the calculated temperature profiles as a function of the residence time for PSR over the same equivalence ratio and pressure ranges. Again, good agreement is observed. It is noted that, while the unstable middle branches of the extinction curve were difficult to obtain using the detailed mechanism, the convergence can be readily achieved using the skeletal mechanism because of the significantly smaller number of system variables. This facilitation in obtaining converged solutions using the skeletal mechanism for applications based on the Newton solver is an extra benefit in addition to the significantly reduced simulation time. The

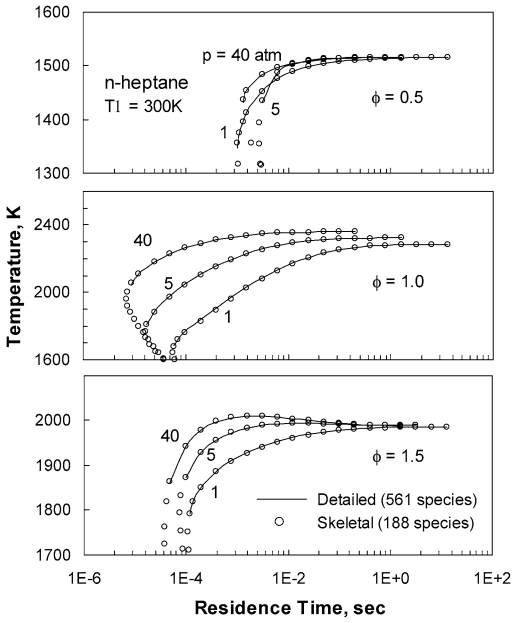

Fig. 6. Comparison of calculated temperature profile in PSR as a function of the residence time for n-heptane/air with the detailed and the 188-species skeletal mechanisms, for equivalence ratio from 0.5 to 1.5, pressure from 1 to 40 atm, and initial temperature 300 K.

good agreement in the comprehensive validation for PSR and autoignition demonstrates the validity of the DRG reduction algorithm.

3.2. Skeletal mechanism for iso-octane

Iso-octane is another important component in fuel blends. It has also been extensively studied experimentally, and many versions of mechanisms for iso-octane oxidation have been developed [26]. While the ignition phenomena for iso-octane bear substantial similarity to those of n-heptane, such as the cool flame and NTC behaviors, the difference in the molecule structure renders the detailed mechanisms for these two large hydrocarbons significantly different from each other. Furthermore, the size of the detailed mechanism for iso-octane is expected to be larger than that of n-heptane. For example, the detailed 2002 mechanism by Curran et al. [26], downloadable from [36], has 857 species and 3606 reactions. While a reduced mechanism for the iso-octane flame structure has been developed based on a much smaller mechanism [37], the comprehensive reduction based on the large mechanism [26,36] is formidable using traditional approaches.

Using the same parameter range and sample applications as those for n-heptane, the detailed iso-octane mechanism was reduced with the two-stage DRG method. Fig. 7 shows the number of species

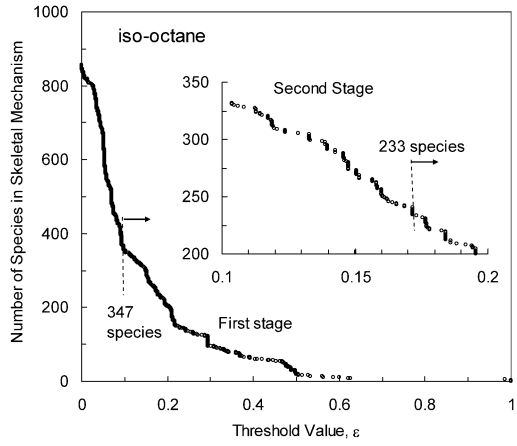

Fig. 7. Dependence of number of species in the skeletal mechanism as a function of the user-specified error threshold value ε for the first and second stages of global DRG reduction for iso-octane mixture, based on densely sampled reactions states from PSR and autoignition for pressure from 1 to 40 atm, equivalence ratio from 0.5 to 1.5, initial temperature range from 600 to 1800 K for autoignition, and 300 K for PSR.

to be retained as a function of the critical value of ε for the first and second reduction stages. By selecting $\varepsilon = 0.1$ for the first stage, a skeletal mechanism with 347 species was obtained for further reduction through the second stage, which subsequently yields a skeletal mechanism with 233 species and 959 reactions. The comprehensive validation of the skeletal mechanism for PSR and autoignition are shown in Figs. 8 and 9, respectively. Close agreement is again observed.

4. Further validation

While the accuracy of the skeletal mechanisms reduced using DRG is bounded by the threshold error value ε, the comprehensiveness is determined by the parameter range and the phenomena based on which the mechanisms are developed. Thus in comprehensive reduction it is necessary to cover the ranges of temperature, pressure, and reactant concentrations as extensively as possible, as has been done in the present study. Furthermore, the selected phenomena are expected to be relevant to more complex phenomena which consist of subregimes with reaction states similar to those covered in the reduction stage. Consequently, we have selected PSR and autoignition, respectively, to capture the high-temperature burning and extinction situations and the low-temperature ignition situations. The reduced mechanisms generated were shown to mimic the detailed mechanisms well for these two phenomena.

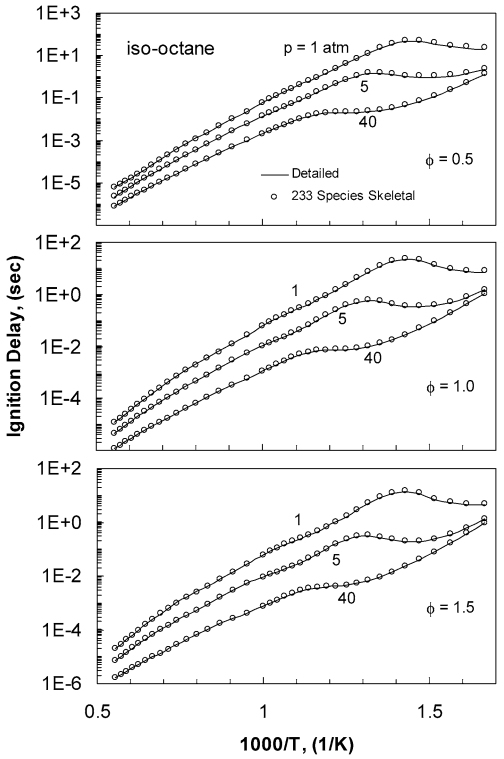

Fig. 8. Comparison of calculated ignition delay for iso-octane/air mixture autoignition as a function of initial temperature under constant pressure and constant enthalpy with the detailed and the 233-species skeletal mechanisms, for equivalence ratio from 0.5 to 1.5, pressure from 1 to 40 atm, and initial temperature from 600 to 1800 K.

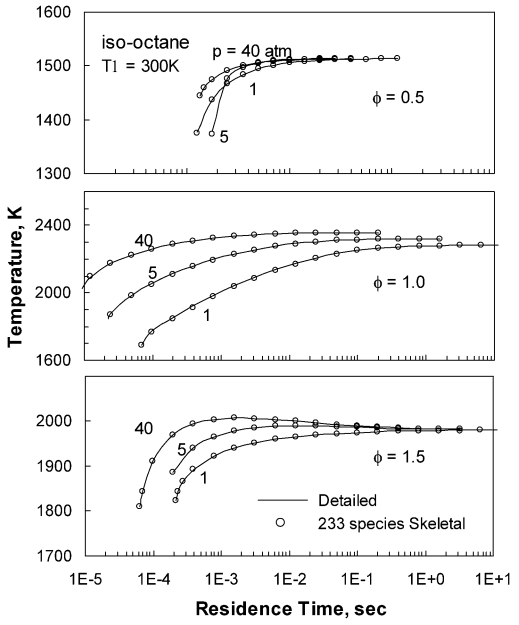

Fig. 9. Comparison of calculated temperature profile in PSR as a function of the residence time for iso-octane/air with the detailed and the 233-species skeletal mechanisms, for equivalence ratio from 0.5 to 1.5, pressure from 1 to 40 atm, and initial temperature 300 K.

The final step in the development of the reduced mechanism is then to apply the reduced mechanisms to phenomena other than PSR and autoignition, for an independent validation. In our previous studies on ethylene [24], we have extended the validation of the performance of the reduced mechanisms to the calculation of diffusive systems involving laminar flame speeds and nonpremixed counterflow ignition. Such a comparison, however, is formidable due to the heavy demand in CPU time for the present large mechanisms. As an alternative, we have selected the response of the jet-stirred reactor (JSR) for an independent validation. This system covers both low- and moderately high-temperature situations, with the presence of combustion-generated radicals to initiate ignition as compared to the need for self-generation in autoignition.

Figs. 10 and 11 show the temperature rise in JSR as a function of the initial temperature of the mixture for stoichiometric 0.1% n-heptane and 0.1% iso-octane mixtures, respectively, with $\phi = 0.5$–1.5, $p =$ 10–40 atm, and residence time $\tau = 1$ s. It is seen that the skeletal mechanisms mostly agree very well with the detailed ones, with only slightly larger deviations in a few situations with maximum errors less than 15%, which is consistent with the assigned accuracy ε. The extension of the skeletal mechanisms developed based on PSR and autoignition to JSR can therefore be considered successful.

The fidelity of the skeletal mechanisms can be further scrutinized by examining the species profiles. Fig. 12 shows the calculated mole fractions of several species as functions of initial temperature of the iso-octane mixture using the 233-species skeletal and the detailed mechanisms in a JSR, for $\phi = 1, 1.5$, $p = 10$ atm, and residence time $\tau = 1$ s. It is seen that the comparison is mostly very close, with the largest error for both the temperature and the species profiles occurring for the fuel-rich case within the temperature range from 900 to 1000 K. The largest error for the species profiles is about 20% for CO_2 around 900 K, which is still comparable to the error in the temperature profile and the critical value of ε.

As a final example of validation comparison, Figs. 13a and 13b, respectively, show the evolution of the mole fractions of selected major and radical species for a stoichiometric 0.1% iso-octane mixture in an atmospheric-pressure flow reactor, with initial temperature 1080 K. Very close agreement is again observed.

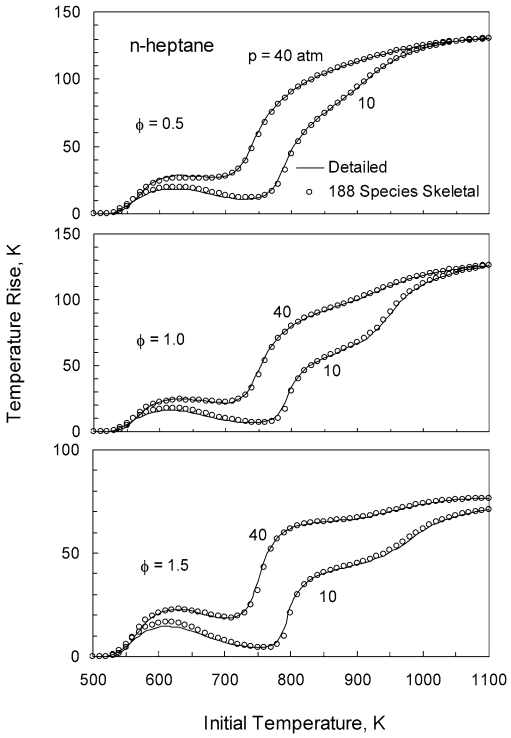

Fig. 10. Comparison of calculated temperature rise in JSR as a function of the initial temperature for 0.1% *n*-heptane with the detailed and the 188-species skeletal mechanisms, for equivalence ratio from 0.5 to 1.5, pressure from 10 to 40 atm, and residence time $\tau = 1$ s.

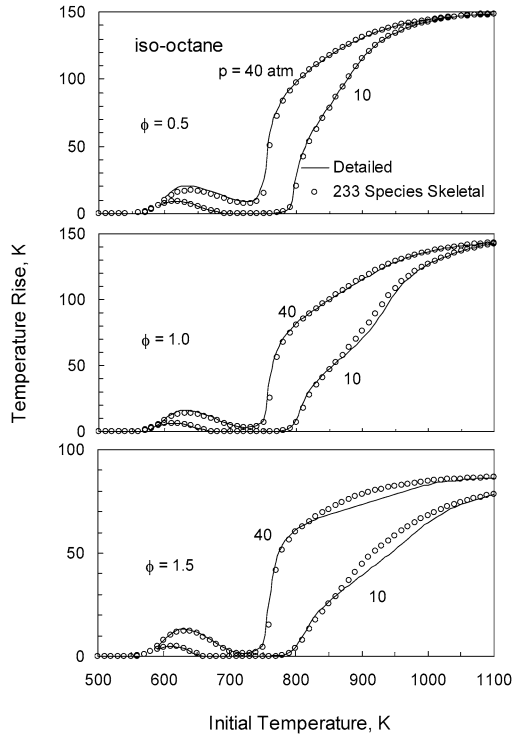

Fig. 11. Comparison of calculated temperature rise in JSR as a function of the initial temperature for 0.1% iso-octane with the detailed and the 233-species skeletal mechanisms, for equivalence ratio from 0.5 to 1.5, pressure from 10 to 40 atm, and residence time $\tau = 1$ s.

5. Error and reduction time

It is noticed from Figs. 11–13 that an important property of the DRG algorithm is that the relative error for each species and major system parameters such as the temperature is equally bounded by the user-specified critical value ε; i.e., every species retained in the skeletal mechanism developed by the DRG method should have an equivalent relative error bound, such that all the species concentrations in the solution should be equivalently trustable. The reason for this merit of the DRG method is that since every species in the dependent set of a species A has to be retained in the skeletal mechanism if species A is kept, as discussed in Section 2.1, the accuracy for every such species A in the skeletal mechanism is therefore bounded by ε.

In developing the reduced mechanism we have required that all sampled states satisfy the critical value ε. The mechanism so derived is therefore comprehensive in its applications, albeit at the expense of keeping more species. It is therefore reasonable to expect that, at the expense of losing some degree of comprehensiveness, a greater extent of reduction can be achieved by performing the reduction locally, say based on reaction states sampled only from the flow reactor configuration. To demonstrate the differences between global and local reductions, Fig. 14 shows the relative error in the temperature rise in a flow reactor for a 0.1% stoichiometric iso-octane mixture under atmospheric pressure with initial temperature 1080 K and residence time $\tau = 0.2$ s. The circles and triangles, respectively, show the relative errors for local and global reductions. For reference, the fractions of eliminated species as functions of the threshold value ε for both the local and the global reductions are shown by the solid curves. It is seen that the relative error for local reduction grows in a linear trend as ε increases, and the line $10 \times \varepsilon$ bounds all the local relative errors. However, the errors for global reduction are much smaller than those of the local reduction, indicating that, by retaining many species that are not important for the local conditions, the relative errors for the global reduction are reduced. This effect can be clearly seen from the two solid curves: the fraction of eliminated species for the global reduction is much smaller than that for the local reduction with the same threshold value ε. Therefore, the accuracy control scheme in DRG reduction is more clearly demon-

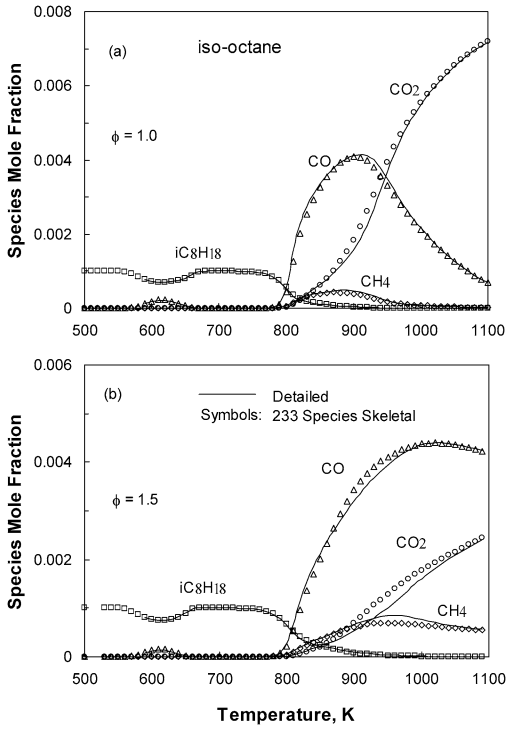

Fig. 12. Comparison of calculated species profiles in JSR as a function of the initial temperature for 0.1% iso-octane with the detailed and the 188-species skeletal mechanisms, for $\phi = 1.0$, $p = 10$ atm, and $\tau = 1$ s.

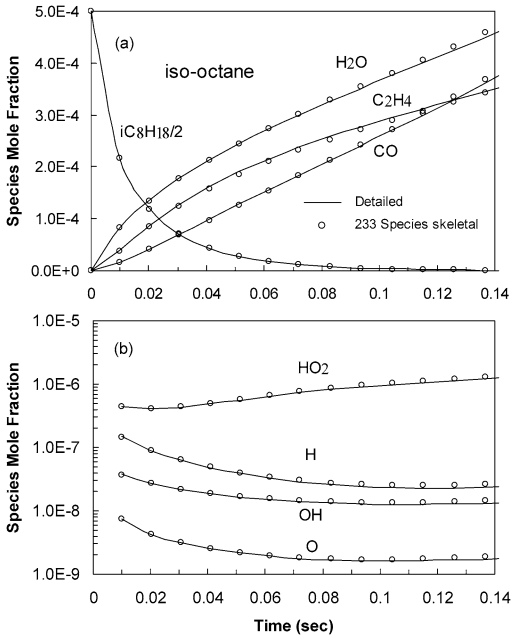

Fig. 13. Comparison of calculated species profiles in a flow reactor as a function of the residence time for 0.1% iso-octane with the detailed and the 233-species skeletal mechanisms, for $\phi = 1.0$, $p = 1$ atm, and initial temperature 1080 K.

strated in the local reduction than in the global reduction. As a result, the ε value describes relative errors better in local reduction than in global reduction. Consequently, the value of ε should be selected conservatively for the local reduction and aggressively for the global reduction. For example, to obtain a skeletal mechanism using local DRG reduction with a relative error tolerance of 10%, a conservative value of $\varepsilon \sim 1\%$ should be used. On the other hand, by using the global reduction with the same error tolerance, an aggressive 10–20% can be selected.

We next investigate the actual time involved in processing the reduction. Fig. 15 shows the measured average local reduction time for a single reaction state as a function of the size of the mechanism, i.e., the number of reactions or number of species in the mechanism. Each data point was averaged from more than 500 local reductions using the reaction states sampled from PSR and autoignition over a parametric range similar to that for the comprehensive reduction for n-heptane and iso-octane in Section 3. Detailed and skeletal mechanisms of various sizes for different fuels were taken as the starting mechanisms for DRG reduction. It is seen from Fig. 15a that the reduction time varies fairly linearly with the number of reactions in the mechanism, as anticipated from the discussions in Section 2.2. Furthermore, the reduction time for the large iso-octane mechanism with 857 species takes only about 50 ms, which is negligible compared to the simulation time and thereby demonstrates the efficiency of the DRG reduction. Fig. 15b shows that the reduction time also varies quite linearly with the number of species in the mechanism. This is possibly a consequence of the practical observation that the number of reactions in large detailed mechanisms is approximately linearly proportional to the number of species.

6. Conclusion

In the present study we have significantly improved the capability of the DRG method for skeletal mechanism reduction. Specifically, overall linear time reduction is achieved by employing a linear time algorithm for graph construction and a revised deep first graph search algorithm. The RDFS algorithm generates all possible skeletal mechanisms ordered by accuracy by a single linear time searching and can be applied for reductions requiring fixed numbers of species in the skeletal mechanism.

The reduction time for large mechanisms was shown theoretically and experimentally to be linearly proportional to the number of reactions in the

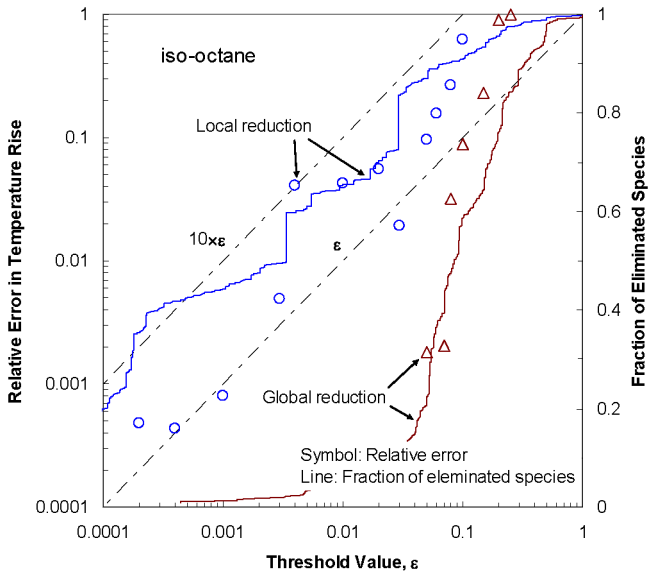

Fig. 14. Calculated relative error in temperature rise for 0.1% iso-octane, as function of the user-specified error threshold value ε, in a flow reactor with $\phi = 1.0$, $p = 1$ atm, initial temperature 1080 K, and residence time $\tau = 0.2$ s, for both local and global reduction.

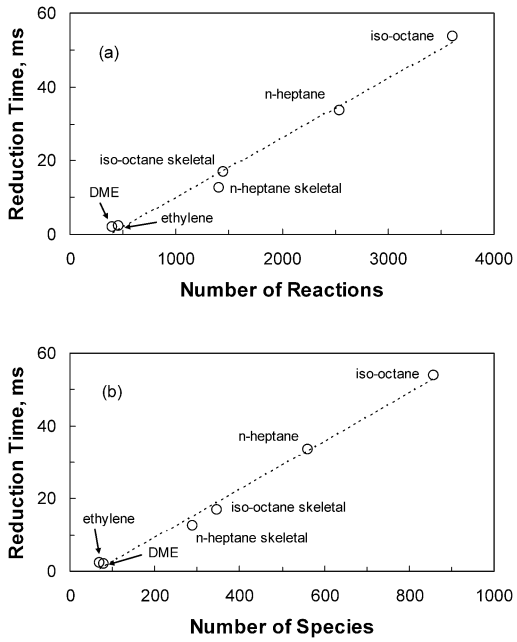

Fig. 15. Measured average reduction time of DRG for a single reaction state as a linear function of (a) number of reactions and (b) number of species of the detailed mechanism.

mechanism. Furthermore, the DRG method exploits a normalized error threshold value which is very easy to specify. Consequently the reduction requires only minimal system-dependent knowledge and the entire reduction process can be fully automated. The high-efficiency and fully automated reduction render DRG particularly suitable for case-specific or real time reduction, in which the reduction time is required to be much shorter than or at least comparable to the simulation time.

The extent of reduction can be further increased, albeit to a much smaller degree, through a second-stage application of DRG and the subsequent application of the CSP importance index.

The usefulness of the present reduction algorithm and strategy clearly increases rapidly with increasing mechanism size. Indeed, this is probably the only approach that can expeditiously and automatically generate skeletal mechanisms from extremely large detailed mechanisms. Specifically, a 188-species and a 233-species skeletal mechanism, respectively, were generated from a detailed 561-species *n*-heptane mechanism and a detailed 857-species mechanism. Not only do these skeletal mechanisms mimic well the responses of autoignition and PSR over extensive parametric ranges, from which they were developed, but the agreement was almost equally satisfactory for the independent system of JSR.

The relative errors for local and global DRG reductions were found to be bounded by a linear function of the accuracy threshold. Furthermore, while the error for the global reduction is much smaller than that of the local reduction, the skeletal mechanism derived with global reduction is much larger. As such, the threshold value employed in mechanism reduction should be selected conservatively for local reduction but aggressively for global reduction.

We close this exposition by emphasizing the high efficiency of the present linear time algorithm, which is responsible for the extremely short time in mechanism generation, as for the case of 50 ms for iso-octane.

Acknowledgment

This work was supported by the Air Force Office of Scientific Research under the technical monitoring of Dr. Julian M. Tishkoff.

References

[1] N. Peters, F.A. Williams, Combust. Flame 68 (2) (1987) 185–207.
[2] K. Seshadri, N. Peters, Combust. Flame 73 (1) (1988) 23–44.
[3] T. Turanyi, A.S. Tomlin, M.J. Pilling, J. Phys. Chem. 97 (1993) 163–172.
[4] J.Y. Chen, Combust. Sci. Technol. 57 (1988) 89–94.
[5] C.J. Sung, C.K. Law, J.Y. Chen, Proc. Combust. Inst. 27 (1998) 295–304.
[6] C.J. Sung, C.K. Law, J.Y. Chen, Combust. Flame 125 (2001) 906–919.
[7] T. Turanyi, J. Toth, Acta Chim. Hung. 129 (1992) 903–914.
[8] H.S. Soyhan, F. Mauss, C. Sorusbay, Combust. Sci. Technol. 174 (11–12) (2002) 73–91.
[9] U. Maas, S.B. Pope, Combust. Flame 88 (3–4) (1992) 239–264.
[10] S.B. Pope, Combust. Theory Modeling 1 (1997) 41–63.
[11] B. Yang, S.B. Pope, Combust. Flame 112 (1998) 85–112.
[12] S.H. Lam, D.A. Goussis, Proc. Combust. Inst. 22 (1988) 931–941.
[13] S.H. Lam, D.A. Goussis, Int. J. Chem. Kinet. 26 (1994) 461–486.
[14] A. Massias, D. Diamantis, E. Mastorakos, D.A. Goussis, Combust. Flame 117 (4) (1999) 685–708.
[15] T.F. Lu, Y. Ju, C.K. Law, Combust. Flame 126 (1–2) (2001) 1445–1455.
[16] M. Valorani, H.N. Najm, D.A. Goussis, Combust. Flame 134 (1–2) (2003) 35–53.
[17] H. Rabitz, M. Kramer, D. Dacol, Annu. Rev. Phys. Chem. 1134 (1983) 419–461.
[18] T. Turanyi, J. Math. Chem. 5 (1990) 203–248.
[19] A.S. Tomlin, T. Turanyi, M.J. Pilling, Comprehensive Chemical Kinetics, Elsevier, 1997, pp. 293–437.
[20] S. Vajada, P. Valko, T. Turanyi, Int. J. Chem. Kinet. 17 (1985) 55–81.
[21] B. Bhattacharjee, D.A. Schwer, P.I. Barton, W.H. Green, Combust. Flame 135 (2003) 191–208.
[22] H. Wang, M. Frenklach, Combust. Flame 87 (3–4) (1991) 365–370.
[23] T. Turanyi, New J. Chem. 14 (1990) 795–803.
[24] T.F. Lu, C.K. Law, Proc. Combust. Inst. 30 (2005) 1333–1341.
[25] H.J. Curran, P. Gaffuri, W.J. Pitz, C.K. Westbrook, Combust. Flame 114 (1–2) (1998) 149–177.
[26] H.J. Curran, P. Gaffuri, W.J. Pitz, C.K. Westbrook, Combust. Flame 129 (3) (2002) 253–280.
[27] http://www-cms.llnl.gov/combustion/combustion2.html#n-C7H16, August 2004.
[28] J.D. Blouch, C.K. Law, Proc. Combust. Inst. 28 (2000) 1679–1686.
[29] A. Chakir, M. Belliman, J.C. Boettner, M. Cathonnet, Int. J. Chem. Kinet. 24 (1992) 385–410.
[30] R.P. Lindstedt, L.Q. Maurice, Combust. Sci. Technol. 107 (1995) 317–353.
[31] T.J. Held, A.J. Marchese, F.L. Dryer, Combust. Sci. Technol. 123 (1997) 107–146.
[32] N. Peters, G. Paczko, R. Seiser, K. Seshadri, Combust. Flame 128 (1–2) (2002) 38–59.
[33] M. Bollig, H. Pitsch, J. Hewson, K. Seshadri, Proc. Combust. Inst. 26 (1996) 729–737.
[34] R. Seiser, H. Pitsch, K. Seshadri, W.J. Pitz, H.J. Curran, Proc. Combust. Inst. 28 (2000) 2029–2037.
[35] S.L. Liu, J.C. Hewson, J.H. Chen, H. Pitsch, Combust. Flame 137 (3) (2004) 320–339.
[36] http://www-cms.llnl.gov/combustion/combustion2.html#i-C8H18, August 2004.
[37] H. Pitsch, N. Peters, Proc. Combust. Inst. 26 (1996) 763–771.